Computers and Electronics in Agriculture 91 (2013) 57–64

Contents lists available at SciVerse ScienceDirect

Computers and Electronics in Agriculture

journal homepage: www.elsevier.com/locate/compag

Estimation of mango crop yield using image analysis – Segmentation method

A.B. Payne [a], K.B. Walsh [b,*], P.P. Subedi [b], D. Jarvis [a]

[a] Central Queensland University, Centre for Intelligent and Networked Systems, Bruce Highway, Rockhampton, Queensland 4701, Australia
[b] Central Queensland University, Centre for Plant and Water Science, Bruce Highway, Rockhampton, Queensland 4701, Australia

ARTICLE INFO

Article history:
Received 11 May 2012
Received in revised form 7 November 2012
Accepted 8 November 2012

Keywords:
Applied image colour segmentation
Processing
Fruit
Automated counting
Texture segmentation

ABSTRACT

This paper presents an approach to count mango fruit from daytime images of individual trees for the purpose of a machine vision based estimation of mango crop yield. Images of mango trees were acquired over a three day period, 3 weeks before commercial harvest occurred. The fruit load of each of fifteen trees was manually counted, and these trees were imaged on four sides. Correlation between tree counts and manual image counts was strong (R^2 = 0.91 for two sides). A further 555 trees were imaged on one side only. For these images, pixels were segmented into fruit and background pixels using colour segmentation in the RGB and YCbCr colour ranges and a texture segmentation based on adjacent pixel variability. Resultant blobs were counted to obtain a per image mango count. Across a set of 555 images (with mean ± standard deviation of fruit per tree of 32.3 ± 14.3), a linear regression, ($y = 0.582x - 0.20$, R^2 = 0.74, bias adjusted root mean square error of prediction = 7.7) was achieved on the machine vision count relative to the image count. The algorithm decreased in effectiveness as the number of fruit on the tree increased, and when imaging conditions involved direct sunlight. Approaches to reduce the impact of fruit load and lighting conditions are discussed.

1. Introduction

Crop yield estimation is carried out in mango orchards 4–6 weeks prior to harvest to predict resource requirements for the harvest and to arrange marketing. Estimation is a manual process, sometimes aided by the use of hand counters. Typically a few 'sentinel' trees are assessed per block, but nonetheless many man hours are required in field conditions of heat and humidity. Ideally, load would be assessed at several times during crop growth but labour requirements prevent this. Further, the sampling procedure limits the accuracy of the process, in terms of estimating the yield of the whole orchard.

A machine vision based system could replace the manual system. Several sensor technologies hold promise for this application, including LIDAR, thermal imaging and stereovision. However, the simplest and lowest cost solution would involve 2D machine vision. A camera mounted to a farm vehicle that drives between tree rows could be used to acquire images of all trees on the farm relatively quickly. An appropriate image processing system would need to be robust in its identification of mango fruit (i.e. require minimal input from farm staff). Further work is required to relate the fruit count from two images of a tree (as seen from the inter-row on each side) to the total fruit load of the tree, a relationship that will vary with canopy architecture. However, given that the intent is to gain an estimate of crop yield to inform harvest decisions, the system does not need to recognise every fruit – an error rate of up to 20% would be tolerable in the first instance.

Once available, a machine vision based system could be used in different ways beyond simply replacing the existing manual fruit count system. Images could be inspected remotely, employing a 'tele-agronomist' approach. Linked to a GPS, farm maps of fruit yield per tree could be implemented, allowing spatially targeted agronomic measures, and removal of underperforming trees. The development of a machine vision system that allows for recognition of fruit is also fundamental to the implementation of robotic harvesting. There is also potential to compare fruit and tree images collected over time. Within season images could potentially be used to assess fruit growth rates, towards a prediction of harvest date. Between season images could be used to assess canopy growth and fruit load capacity on an individual tree basis.

The purpose of this paper is to describe an image processing technique to count the number of fruit within an image of a (mango) tree, from an RGB image.

Machine vision has been extensively employed in fruit pack-lines since the 1970s (e.g. Herold et al., 2009). However, the use of machine vision for fruit counting in an orchard presents many challenges relative to the structured (in background, lighting, etc.) conditions of a fruit pack-line. Daytime lighting can be bright, strong, directional and variable, the more so in the tropical environments in which mango are grown. As noted by Tews et al.

* Corresponding author. Tel.: +61 7 49309707; fax: +61 7 49306536.
E-mail address: k.walsh@cqu.edu.au (K.B. Walsh).

0168-1699/$ - see front matter © 2012 Elsevier B.V. All rights reserved.
http://dx.doi.org/10.1016/j.compag.2012.11.009

(2005), inconsistencies created by direct and reflected illumination from the sun and clouds, and the extent of shadowing on the subject complicate the image processing task. The on-tree task is also challenging in terms of the similarity of the background to the object of interest (e.g. green fruit against green foliage) and foreground complications (e.g. leaves that cross in front of the fruit, breaking its oval silhouette). Within this environment, the first image processing step is to segment the fruit from the background. A range of colour spaces and techniques have been used across different types of fruit, as reviewed in brief in the following text:

An on-tree count of apple fruit was considered using a combination of thermal and RGB images by (Stajnko et al., 2004). The use of normalised chromaticity coordinates (R, G, and B) to reduce the effect of lighting variation was insufficient to segment all pixels accurately. They then used a normalized difference index (NDI).

$$NDI = \frac{G - R}{G + R} \quad (1)$$

This index separated a majority of the pixels well, but a further erosion step was used to create the final segmentation. Using feature extraction, particle selection and classifier evaluation, they identified and counted fruit, achieving an R value between 0.70 and 0.88. The correlation coefficients for the average yield per tree increased with the ripening of fruit from 0.28 through to 0.87 as a result of the increasing colouration of the fruit.

Later work by this group (Stajnko et al., 2009) used colour features and surface texture to segment fruit from background. The use the HIS colour space to segment fruit from background was based on empirically determined segmentation thresholds. In this work, the magnitude of red colour intensities ($R\_I = 3{*}R{-}B{-}G$) was calculated, followed by average contrast, uniformity and average entropy. Pixels which remained in each of these steps formed a cumulative image for further consideration. They then performed shape reconstruction, seeking prominent circular regions. Fruit detection rates were high (89%), with low error rates (2.2%).

(Zhou et al. (2012)) also used colour (RGB/HSI space) to detect both green and red apples on tree. They used colour difference (red–blue and green–red) to develop a colour model to threshold the fruit. By thresholding and comparing using these values, they progressively removed background pixels, and became more specific in their detection of fruit pixels. For red apples, they converted to HIS space and selected pixels based on the saturation layer. They obtained high correlation coefficients ($R^2 = 0.80$ and 0.85) for particular development periods.

Citrus fruit on tree has been considered by a number of authors, particularly of fully mature and well coloured fruit (as the orange coloured fruit contrast well to the green foliage background). Regunathan and Lee (2005) differentiated fruit pixels from background pixels using hue and saturation as the separation features. They compared three different classification techniques – Bayesian, neural network and Fischer's linear discriminant. Images had, on average, 37.6 fruit with a standard deviation of 11.4. The root mean square error for the three classifiers used was 4.2, 2.6, and 7.2 respectively. They noted that errors were introduced by variable illumination.

Hannan et al. (2009) worked to improve machine recognition of orange citrus fruit on tree. They found that the red chromaticity coefficient ($R/(R + G + B)$) could be used to enhance the fruit image, which enabled segmentation under variable outdoor illumination. Ninety percent of the fruits were detected, with a false detection rate of 4%. Chinchuluun et al. (2009) photographed citrus on a catch and shake harvester under controlled lighting conditions. They applied a Bayesian classifier to segment fruit and background on the conveyer, and set probabilities from a sample set of 60 images. The discriminant function was based on I (YIQ) and hue (HIS) components of the image. An R^2 value of 0.891 between the actual and estimated number of fruit was achieved.

Billingsley (2006) described a machine vision system to count macadamias on a harvester roller. A colour discrimination step was used (red > blue) to separate nuts from the (blue) roller.

Widjethunga et al. (2008) investigated image analysis techniques to automate kiwifruit counting in images of fruit on vine (with camera looking vertically up at hanging fruit). They created a false colour image in which kiwi fruit were prominent through modification of the image intensity, removal of the G band, and emphasis of the B band of the RGB photo. They then altered the colour space of this false colour photograph to $L{*}a{*}b$, and used $a{*}$ and $b{*}$ attributes to segment the photo into four regions, including a kiwi fruit region. As the kiwifruit centre had a comparatively higher grey value, they could use regional maximums to identify and count the fruit. They achieved 90% accuracy on fruit of the Gold variety and 60% accuracy on the standard green Hayward variety.

Patel et al. (2011) offer a comprehensive approach to fruit detection using multiple features. They employed colour, orientation and edge feature extraction prior to combining the results to perform segmentation of fruit from background. They noted that this approach has general applicability, and presented examples of segmentation for ten different types of fruit. Using the approach, they correctly detected 95% of the fruit pixels within a photograph. However, they made no attempt to count the fruit, or apply the work to multiple images collected under different lighting conditions.

There are a range of other image processing techniques which may be applied to crop yield estimation. A recent review of those used in plant disease detection (Patil and Kumar, 2011) discusses a large number of techniques, including neural network based classifiers, principal components assessment (PCA), expert systems and a variety of segmentation techniques. Impediments to their implementation in the area of mango crop yield estimation include the range of lighting conditions in field, variety in tree structure and bearing habit, and variation in fruit colour and difficulty of detection during the course of the mango season, and the number of sample photos required for neural network training.

In human vision of a mango tree canopy, the fruit is recognised by virtue of a combination of the following characters: (i) ovoid shape (or curved edge, where part of the fruit is obscured); (ii) smooth surface; and (iii) skin colour (reddish blush, if present, or a green paler than foliage). Note, however, the shape of the mango fruit is not a simple sphere or ovoid (unlike, e.g. an orange fruit), such that the 2D projection of the fruit in an camera image can take several shapes, and the fruit skin colour can vary, as mentioned. Thus the imaging processing task for recognition of mango fruit within a canopy image is rather more difficult than that of, e.g., recognition of mature oranges.

An additional common problem in fruit detection is that of partial occlusion and clustering of fruits. Hannan et al. (2009) used a perimeter-based detection method to detect citrus fruit in clusters. This approach enhanced results for images acquired under variable lighting conditions and where occlusion existed. Billingsley (2006) used a simple circle-detection algorithm to make final discrimination between macadamia nuts and leaves. These approaches are very relevant to the application of identification of mango fruit within an image of a mango tree canopy, as the fruit is often occluded by leaves or stems, and is often clustered with other fruit (e.g. Fig. 1).

Based on this previous work, a machine vision approach to the detection of mango fruit in images of the whole tree canopy was based on image segmentation based on colour and texture. Additional work was undertaken to test the relationship between image count and total tree fruit count, for the trees considered in this study.

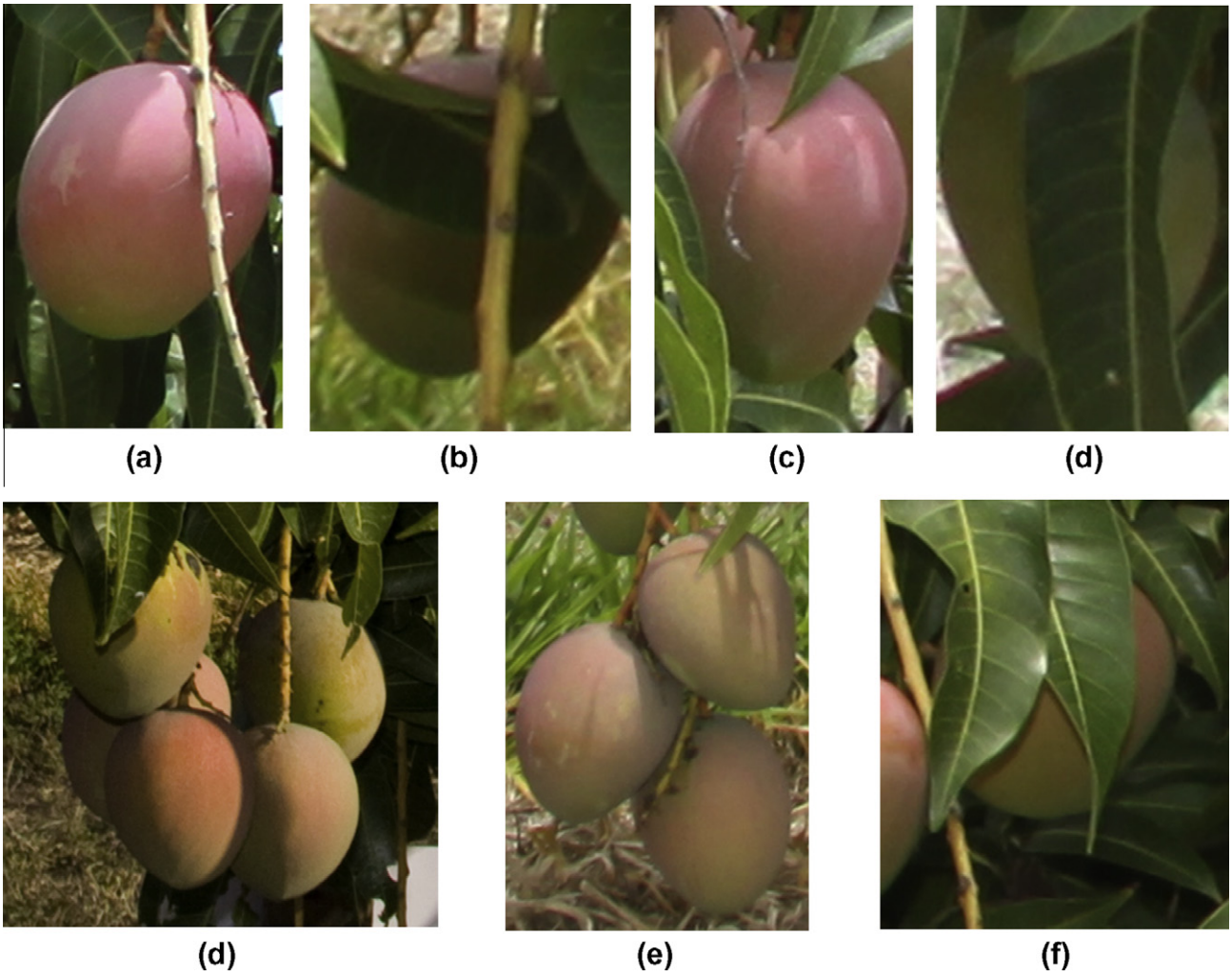

Fig. 1. Examples of lighting condition and fruit occlusion within images: (a) partly shaded fruit 'bisected' by stalk, (b) fully shaded fruit image dissected by leaf and stalk, (c) fruit partly visible, obscured by leaf and stalk, (d) shaded fruit dissected by leaf, (e) cluster of fruit with overlapped margins, (f) cluster of fruit with minimal overlap and (g) heavily obscured fruit.

2. Materials and methods

Images were collected of 593 trees in a large North Queensland mango orchard of 56,000 trees (approximately 1% of the orchard), 3 weeks after the 'stone hardening stage' of fruit development and approximately 3 weeks before harvest in late October, 2010. The trees imaged were randomly selected from a number of blocks within the orchard, in an attempt to include variation in canopy structure (which affects the extent of fruit occlusion) and plant nutrition (which affects leaf and fruit colouration). Trees were imaged over three days. On day 1, 38 trees were imaged on day on all four sides (image set 1). Over the next 2 days, a further 555 trees were imaged on only one side (image set 2). Trees were approximately 2–3 m in height, and fruit generally displayed a strong blush (skin colouration association with fruit maturation).

A manual count of all fruit which had reached maturity (stone hardening) for the first 15 trees imaged on day 1 was undertaken by a single human operator.

Images were acquired using a tripod mounted Canon 50D SLR camera using a 28–135 mm zoom lens. The camera was positioned approximately 2 m from the tree trunk, and at a position in the inter-row perpendicular to the position of the tree in the row. Each image presented a single tree in its' centre, with background consisting of grass, sky, other orchard trees and occasionally machinery and people (Fig. 2). Images were stored in JPG format in RGB colour and at a resolution of 4752 × 3168 pixels (Canon 50D large format at approximately 5 Mbytes per photo). Images were acquired during the morning on day 1 (8.50 am–12.30 pm),

Fig. 2. Example image of mango tree in orchard, photographed from the inter-row.

and for days 2 and 3 during the middle of the day (between 2.30 and 3.45 pm on day 1, and 10.10–12.40 pm on day 2).

The JPG format is not ideal for image processing being a lossy format, and the use of the camera RAW format and lossless TIFF for processing is recommended. However, initial results with these lossless image formats suggest that there has been little impact on results by using the high quality JPG format.

Images were opened in Adobe Photoshop, and the built in Count Tool was used in manually tally the number of fruit on the tree in the image (examined at a 3× magnification). The image fruit count was exhaustive, including any fruit which could be identified by the human eye, no matter how obscured. Approximately one-third of the fruit were clearly visible and largely unobscured. Slightly less than one third of all fruit were over 95% obscured. Fallen fruit and fruit which were clearly damaged, showing significant yellowing, blackness or a shrivelled appearance, were excluded from this count. The average number of fruit per tree (image set 2) was 32.3, with a standard deviation of 14.3.

The lighting conditions on day one of collection was strong, bright sunshine. On both following days of image collection, the sky was overcast, with intermittent periods of bright sunshine and diffuse lighting conditions. Images collected were classified based on the lighting conditions into the categories of bright lighting (strong shadows visible, e.g. Fig. 2), moderate lighting (some shadow apparent), and diffuse lighting conditions (no shadow). For image set 1, there were 12 (7.9%) diffuse images, 12 (7.9%) moderate sunlight images, and 128 (84.2%) bright condition images (Table 1). For image set 2, there were 242 (43.5%) diffuse images within the set, 94 (16.9%) moderate sunlight images, and 220 (36.9%) bright condition images (Table 2).

Images in set 1 and set 2 were also classified based on fruit load per tree. Trees with a fruit number within one standard deviation of the mean (based on image set 2) were considered to be carrying an 'average' fruit load (18–46 fruit). Those carrying less than 18 fruit were considered to be carrying a 'low' fruit load, and those above 46 fruit were deemed to carry a 'high' fruit load. In set 1, there were 8 (5.3%) trees carrying a low fruit load, 64 (42.1%) trees carrying an average fruit load, and 80 (52.7%) trees carrying a high fruit load (Table 1) In set 2, there were 85 (15.3%) trees carrying a low fruit load, 389 (70.1%) trees carrying an average fruit load, and 81 (14.6%) trees carrying a high fruit load (Table 2).

The program for automated fruit count was developed using ImageJ Version 1.44p. The RGB image was transformed to create a number of different colour and intensity views of the tree. A number of colour spaces were considered prior to choosing the Cb and Cr layers of the YCbCr space. These included HSV and CIE Lab. Using empirical testing and visual inspection (using images from set 1), the Cb and Cr layers showed the best differentiation between fruit and background.

Table 1
Set 1. Characterisation of lighting conditions and fruit load per tree, expressed as an absolute number of images and % of all images acquired. Images with less than 18 fruit per image were classified as 'low' load, between 18 and 47 an 'average' load, and above 47, as 'high' load. These values were chosen as one standard deviation above and below the mean for the image set (555 trees) from image set 2 with a mean of 32.3 and a standard deviation of 14.3.

Characteristics		Fruit load (% of total)			All loads
		Low	Average	High	
Lighting conditions	Diffuse	0 (0%)	4 (2.6%)	8 (5.3%)	12 (7.9%)
	Moderate	0 (0%)	4 (2.6%)	8 (5.3%)	12 (7.9%)
	Bright	8 (5.3%)	56 (36.8%)	64 (42.1%)	128 (84.2%)
	All conditions	8 (5.3%)	64 (42.1%)	80 (52.7%)	152 (100%)

Table 2
Distribution of image set 2 ($n = 555$) by lighting condition and fruit load per tree (presented as absolute number of images, and as percentage of total images).

Characteristics		Fruit load			All fruit loads
		Low	Average	High	
Lighting conditions	Diffuse	37 (6.67%)	174 (31.4%)	31 (5.6%)	242 (43.6%)
	Moderate	18 (3.2%)	63 (11.4%)	12 (2.2%)	94 (16.8%)
	Bright	30 (5.4%)	152 (27.4%)	38 (6.9%)	220 (39.6%)
	All conditions	85 (15.3%)	389 (70.1%)	81 (14.6%)	555 (100%)

These views used in image segmentation were:

(i) The original RGB photo.
(ii) The red layer of RGB (R).
(iii) The green layer of RGB (G).
(iv) The RGB photo was transformed into YCbCr colour space, and the Cb layer (Cb; blue difference chroma component) selected.
(v) From the YCbCr colour space, the Cr layer (Cr; the red difference chroma component) was selected. The criterion set on conditions for each step was adjusted based on empirical testing and visual inspection using the 38 images from set 1. Algorithm performance was assessed in terms of R^2 and root mean square of errors of prediction (RMSEP) for the set of 555 images.

A subset of 60 images from set 2 was used in characterisation of the types of errors incurred in the machine analysis (both in terms of false positive and negative identification of image areas as fruit). This subset was the first 60 images collected in set 2.

3. Results

3.1. Tree load compared with image counts

The linear correlation between a manual count of fruit in images of the various sides of 15 trees and a manual count of the total number of fruit on each of the trees was generally strong, with an R^2 value of between 0.81 and 0.93 for a single side, 0.91 for addition of counts from opposing sides, and 0.93 for a count involving all four sides (Table 3). Because many fruit hang below the canopy, and are visible from any side of the tree, side A image count was 80 ± 22% (mean ± SD) of actual tree fruit load f, while side $A + C$ count was 150% of tree count and side $A + B + C + D$ count was 167/62% of tree count.

3.2. Algorithm

A method for automated recognition of fruit within an image was developed, based on the features used in human vision (viz. texture and colour). The first stage in recognition of a mango fruit

Table 3
Manual count of fruit per tree and in images taken from four aspects of each tree (data of 15 trees). Linear regression coefficient of determination between image count and total fruit per tree is also recorded.

Sample #	Fruit # per tree	Side (s)						
		A	B	C	D	$A + C$	$B + D$	$A + B + C + D$
Mean	61.7	45.7	38.1	44.1	39.3	89.9	77.4	167.3
SD	29.6	20.8	15.4	18.5	17.1	38.1	31.9	69.2
R^2		0.83	0.81	0.88	0.93	0.91	0.91	0.93

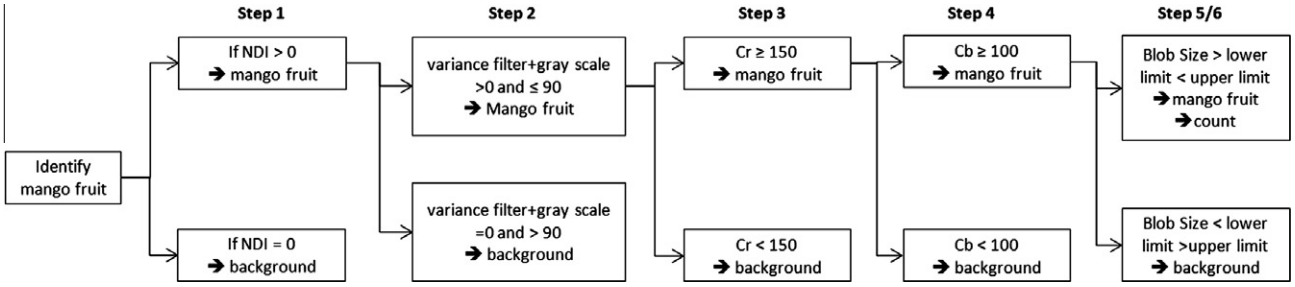

Fig. 3. Outine of the processing steps in the algorithm.

within the image was to extract features in the RGB and YCbCr colour spaces, using these features to eliminate or include a pixel in a binary mask of the image. Simple binary particle analysis was then carried out on this binary image in order to provide a count of the mangoes within the picture. The following steps were followed in this procedure, with settings on the filters optimised by an iterative approach (also shown in Fig. 3):

Step 1: The Normalised Difference Index (Eq. (1)) used by Stajnko et al. (2004) was calculated from the R and G layers for each pixel using the following equation. Pixels where $NDI > 0$ were selected.

$$NDI = \frac{G - R}{G + R} \quad (1)$$

This step has the effect of selecting pixels in which red is more dominant than green, thus selecting 'blush' areas of fruit, in preference to foliage.

Step 2: The RGB photo was processed using a 3×3 variance filter which replaces each pixel with the neighbourhood variance of the R, G and B layers respectively. The image was then converted to gray scale using the formula gray = $(R + G + B)/3$. It was then thresholded, using the condition $0 < pixelvalue \leqslant 90$.

This step effectively removes pixels which were in regions with a large number of edges – such as within grass or foliage, and also pixels where there was little variance, such as sky.

Step 3: The Cr layer was thresholded, using the condition of $Cr \geqslant 150$. This value was shown to consistently remove brown grass and tree trunk from the photo, thus reducing background error rates significantly. In late season photos, a majority of mangoes were also retained in the photo given their very strong pink blush.

Step 4: The Cb layer was thresholded using the condition of $Cb > 100$. Fruit and yellow leaf pixels in the Cb layer exhibited a very strong bipolar distribution, and the selection of 100 as a cut-off point was clearly within a wide gap between the two pixel types.

Step 5: A binary image was generated by collating the results of the previous four steps as follows:

$$pixel_{finalimage} = pixel_{NDI} \text{ and } pixel_{variance} \text{ and } pixel_{Cr} \text{ and } pixel_{Cb}$$

The result was a binary image, effectively masking mango regions within the photo.

Step 6: A count of the number of particles in the binary image was performed. Particles counted were limited by both a lower and an upper limit on the number of pixels in the particle. The lower limit served to remove fruit on background trees, and some grassed areas which were relatively smooth and pink. This lower limit also had the effect of rejecting some fruit particles, where the fruit was divided because of occlusion. Conversely, a number of fruit were detected twice due to their areas being split by other mango stalks or leaves. The upper limit was set to remove very large false positives in (red soil) road areas which were over-exposed by sunlight and had lost their pattern, and thus were missed in Step 2. The upper limit also had the effect of rejecting some fruit particles, where several fruit were overlapped.

This step provided the final count of mangoes within the photo. The results of each step can be seen in Fig. 4.

Step 2 eliminated sharp edges from consideration as fruit pixels, and thus provided a mechanism to differentiate overlapped fruit. However, there are still a number of examples of overlapping fruit being counted as a single fruit (4.5% of detections).

3.3. Image counts compared with automated counts

Automated and exhaustive manual image counts were compared for the set of 555 mango tree images (set 2; Fig. 5). The average number of fruit in photos was 32.3 with a standard deviation of 14.3. The automated count consistently underestimated the true fruit load (regression slope of 0.58), but an R^2 of 0.74 was achieved. The bias adjusted root mean square error of prediction on the automated count was 7.7.

The coefficient of determination (R^2) of the machine count against the manual count was similar under the three lighting conditions, however, the efficiency of detection (slope) decreased under strong sunlight (Fig. 6).

Algorithm performance also decreased as the number of fruit on the tree increased (Fig. 7b). Indeed, the efficiency of detection was very poor for the high fruit load category of tree (coefficient of determination (R^2) of 0.06, Fig. 7c).

The types of error present in the machine vision analysis were characterised within a set of 60 images (a subset of set 2, the initial 60 trees imaged), containing 2236 mangoes (as estimated by manual count) (data not shown). There were 1209 objects detected by the machine vision procedure. Of the 1209 detected objects, 29 were false detections, an error rate of 2.4%. These false positives were often fruit in the background trees of the photo. Additionally, 29 detections were a second detection of a fruit which was split by stem or leaf. A further 54 (or 4.5%) of the detected objects involved two or more fruit counted as a single fruit, representing missed opportunities to detect, rather than false detections. The most frequent error was that of the failure to detect a fruit that was occluded by a leaf or stem, such that the image of the fruit was broken into smaller units. Thus, in these images, only 51% of the fruit ((1209-29-29)/2236) were correctly detected.

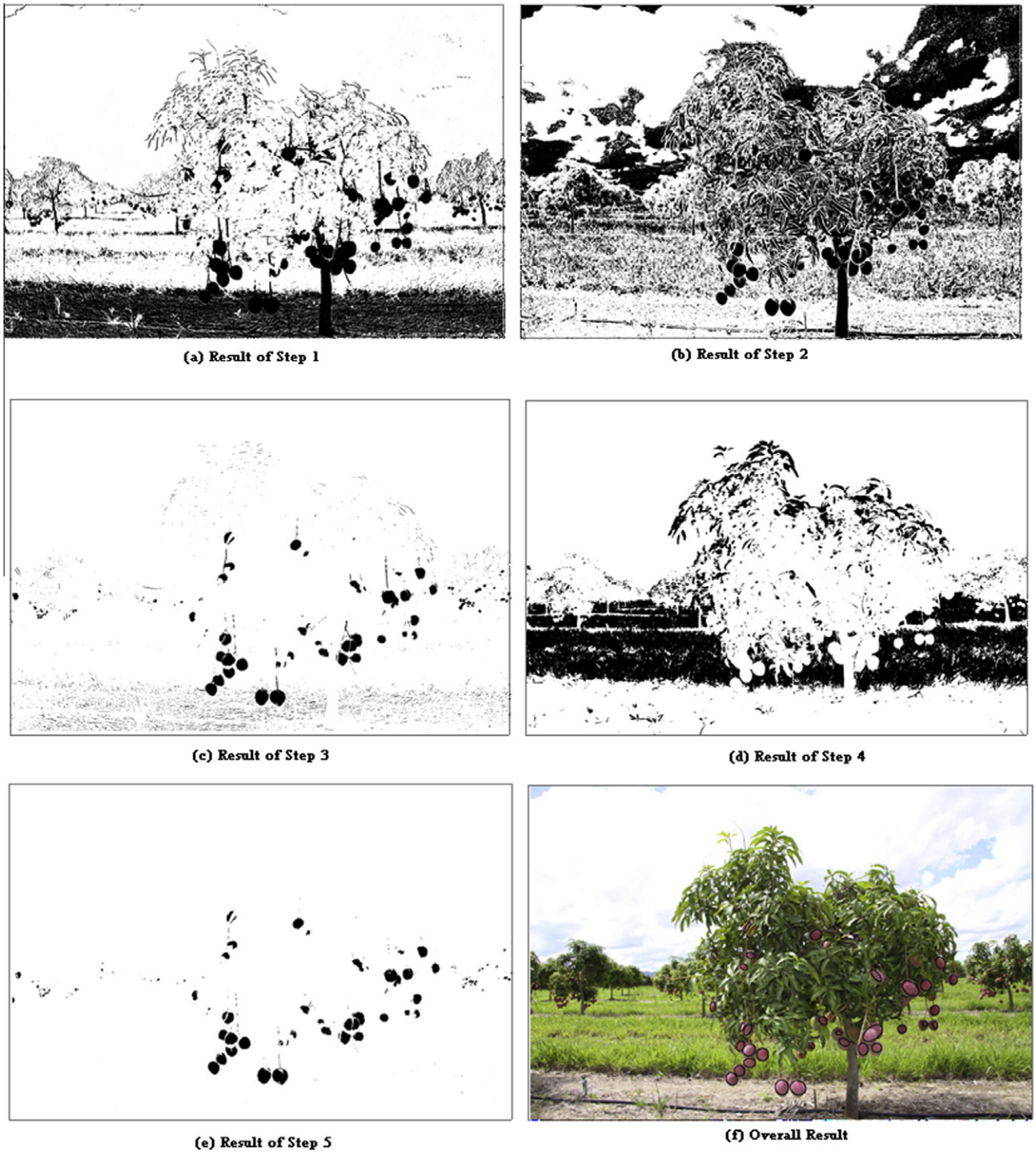

Fig. 4. An example image passed through the six processing steps to identify fruit within the image.

4. Discussion

4.1. Estimating total orchard fruit load

Current industry practice involves assessment of average fruit number across a small (e.g. four) number of trees per block of 1000 trees, with this average multiplied by the number of trees in the block to attain an estimate of fruit load. However, as documented in the exercises above, fruit load per tree is relatively high, and variable.

For a population with a standard deviation on fruit load per tree of 29.6 fruit per tree (Set 1), an appropriate sample size (for 95% confidence) would be 141 (using Eq. (2) below, where n is the required number of samples, s_d is standard deviation and d is the acceptable margin of error, e.g. 5 = 95% confidence) (Gerstman, 2003).

$$n = \frac{4s_c^2}{d^2} \tag{2}$$

Use of only four samples results in an uncertainty of 29.6 (i.e. confidence level of 70.4%). In summary, machine vision can allow improved estimation of orchard yield through a greater sample number, compromised by error in the machine vision count.

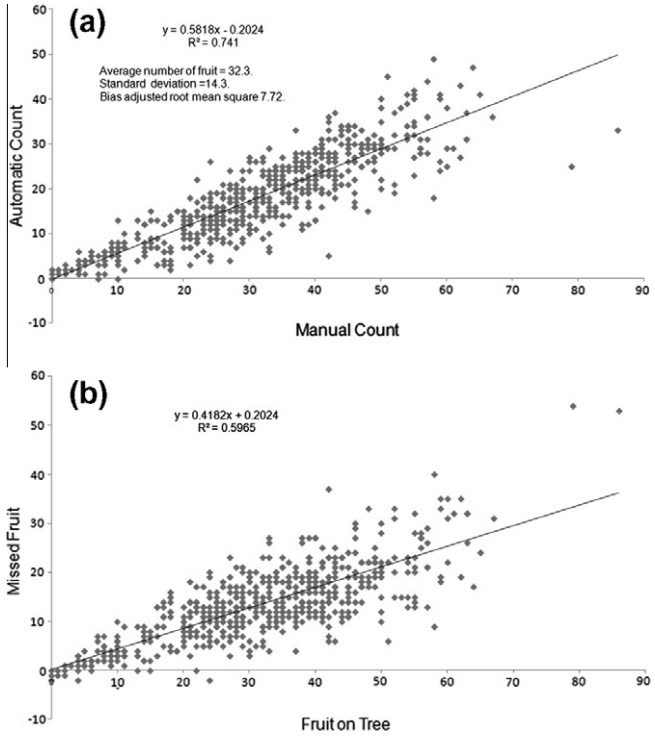

Fig. 5. (a) Plot of automated count against manual count of number of fruit on each on 555 images of mango trees. (b) Number of fruit per image not detected by the machine vision algorithm in relation to fruit load.

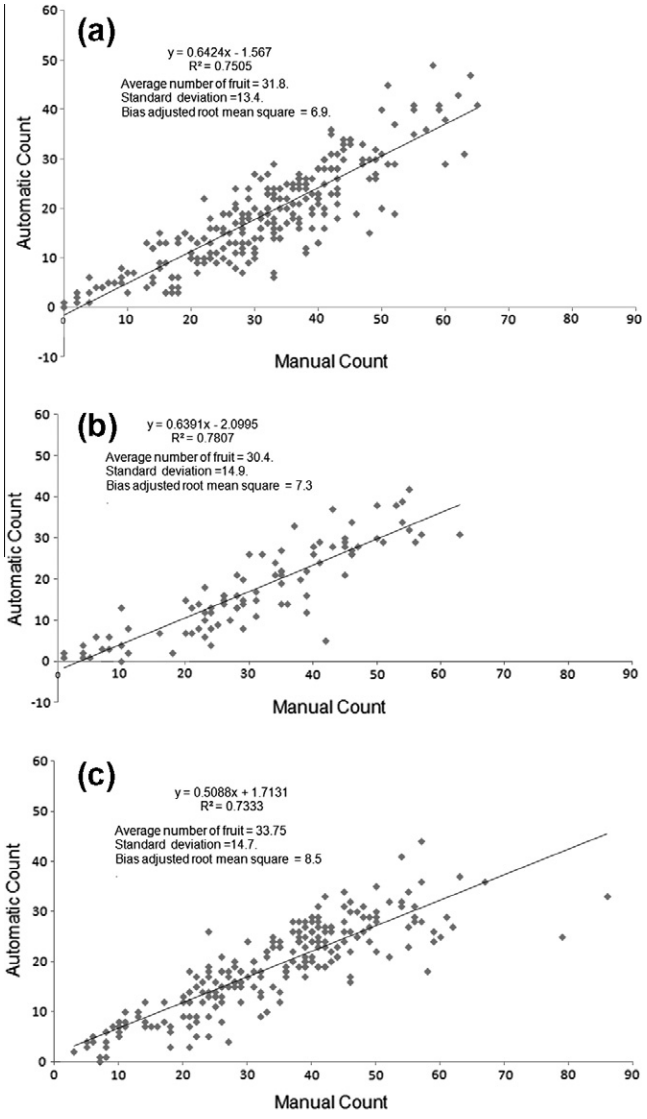

Fig. 6. Plot of automated count against manual count of number 472 of fruit under different lighting conditions: (a) overcast conditions, (b) 473 moderate sunlight, (c) full sunlight.

4.2. Estimating total fruit load from 2D images

Fruit load can be quite different on different sides of a tree. Therefore 2D images from several aspects of the tree were expected to be required to capture information on all fruit on a tree. Images of two sides of the tree, as seen from the inter-row, were sufficient to obtain an estimate of the overall tree fruit load (R^2 value of >0.91, albeit with a significant bias). Of course, this conclusion is specific to the canopy shape and fruit load distribution of this particular population. In practice, this relationship should be established for a given orchard, and re-established following growth or severe pruning of the tree canopy. It is likely that increased orchard automation (in the future) will drive the use of possibly less productive (fruit per ha) but more easily managed canopy architectures (e.g. a planar canopy).

4.3. Estimating total fruit load from automated counts

Image segmentation using colour spaces was difficult for mango fruit, relative to a well coloured fruit contrasting to a green background (e.g. mature citrus). The individual mango fruit vary in colour, from completely green through partly green, and from partly pale orange or reddish colour, to fully yellowish-orange. The green colour of fruit can overlap with leaf colour. Even those varieties with a consistent colour 'blush' at the time of harvest can have significant variation in fruit colour at the point of fruit count earlier in the season, and while the blush colour of fruit is distinctive within the tree, its colour range can be overlapped with background features, such as red soil.

Fruit recognition based on surface texture of areas of appropriate (fruit) was compromised by instances in which the fruit was dissected by an overlying object (leaving areas of uniform texture too small to be recognised as fruit), or by the presence of sky, soil or trunk of uniform texture, and present in patch sizes equivalent to that of fruit (e.g. sky patch bounded by foliage).

The combination of texture and colour filters went some way to eliminating false positives in the identification of fruit. As expected, the adjustment of filter settings to reduce false positives was accompanied by an increase in the failure to recognise fruit in the image (data not shown). Increasing the size of particles recognised has the effect of reducing detected background fruit (i.e. decreased false positives), but also results in elimination of highly obscured fruit on the tree (decreased true positives). The reported filter settings were chosen to keep false positives below 2.5% of all fruit counts.

Across the set of 555 images, an R^2 of 0.74, bias adjusted RMSEP = 7.7, was achieved between automated and manual counts. The automated count was an underestimate of the manual (actual) count, particularly in canopies with higher fruit loads. This trend was a function of the increasing number of partly occluded fruit as canopy load increased.

Lighting conditions affected the quality of results. Diffuse (overcast) conditions produced better results than full sunlight. For example, better algorithm prediction results were obtained with

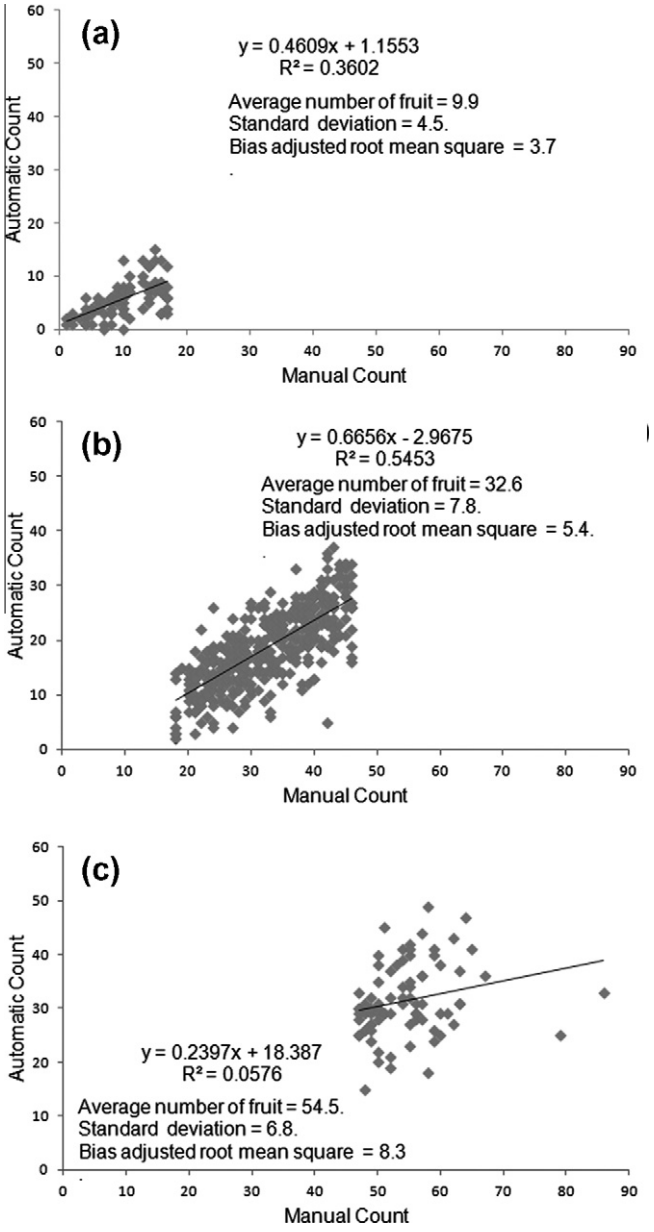

Fig. 7. Plot of automated count against manual count of number of 476 fruit for trees with different fruit loads: (a) low load, (b) moderate load and (c) high load.

set 2 than with set 1, although set 1 was used establishing algorithm settings. Set 1 was obtained on a day of strong sunlight, set 2 on a day with diffuse lighting. The effect of strong sunlight on imaging is probably due to the increasing shadows on fruit under strong illumination – the fruit are therefore split into multiple smaller segments by the algorithm and 'lost' in processing. However, it is not practical to align a counting process with particular weather conditions. For this reason, further investigation of approaches to create consistent lighting conditions is required. Solutions may exist for either day or night photography using artificial lighting.

The application of this work to mango fruit at an earlier stage of fruit development will also offer further challenges, given the lack of blush colour development on less mature fruit. It is expected that the Cr colour range will need to be widened significantly to pick up early season mangoes. This will increase both error rates, and the effect of imperfect lighting conditions.

5. Conclusions

The results presented here are encouraging that a machine vision based mango crop load estimator is possible. However, the development required is significant, particularly for application to less mature fruit, with less fruit colouration. Further work should decrease the emphasis on colour segmentation, consider the use of perimeter matching as a means to improve fruit detection, and should also investigate approaches to establishing consistent lighting conditions in field conditions.

Acknowledgement

This research was funded by Horticulture Australia Limited (HAL) under project HAL Agreement HG08075.

References

Billingsley, J., 2006. More machine vision applications in the NCEA. Proceedings of M2VIP 2006. In: 13th International IEEE Conference on Mechatronics & Machine Vision in Practice, Toowoomba QLD, Australia. ISSN: 1908-1162.

Chinchuluun, R., Lee, W.S., Ehsani, R., 2009. Machine vision system for determining citrus count and size on a canopy shake and catch harvester. Applied Engineering in Agriculture 25 (4), 451–458.

Gerstman, Burt, 2003. Statistics Primer. Versiopn 6.4. from San Jose University: <http://www.sjsu.edu/faculty/gerstman/StatPrimer/samplsize.PDF>. (Retrieved 23.05.2012)

Hannan, M.W., Burks, T.F., Bulanon, D.M., 2009. A machine vision algorithm combining adaptive segmentation and shape analysis for orange fruit detection. In: Agricultural Engineering International: CIGR Journal. (Manuscript 1281). vol. XI, <http://www.cigrjournal.org/index.php/Ejounral/article/view/1281>.

Herold, B., Kawano, S., Sumpf, B., Tillmann, P., Walsh K.B., 2009. VIS/NIR Spectroscopy. In: Zude, M., (Ed.), Optical Monitoring of Fresh and Processed Agricultural Crops, CRC Press Boca Raton USA, ISBN 978-1-4200-5402-6, pp. 141–249, (Chapter 3).

Patel, H.N., Jain, R.K., Joshi, M.V., 2011. Fruit detection using improved multiple features based algorithm. International Journal of Computer Applications 13, 1–5.

Patil, J., Kumar, R., 2011. Advances in image processing for detection of plant diseases. Journal of Advanced Bioinformatics Applications and Research 2, 135–141.

Regunathan, M., Lee, W. S., 2005. Citrus Fruit Identification and Size Determination Using Machine Vision and Ultrasonic Sensors. ASAE Paper number 053017.

Stajnko, D., Lakota, M., Hocevar, M., 2004. Estimation of number and diameter of apple fruits in an orchard during the growing season by thermal imaging. Computers and Electronics in Agriculture 42, 31–34.

Stajnko, D., Rakun, J., et al., 2009. Modelling apple fruit yield using image analysis for fruit colour, shape and texture. European Journal of Horticultural Science 74 (6), 260–267.

Tews, A., Roberts, J., Usher, K., 2005. Is the Sun Too Bright in Queensland? An Approach to Robust Outdoor Colour Beacon Detection. In: Proceedings of the Australasian Conference on Robotics and Automation. Sydney, Australia. <http://www.araa.asn.au/acra/acra2005/papers/tews.pdf>.

Widjethunga, P., Smarasinghe, S., Kulasiri, D., Woodhead, I., 2008. Digital image analysis based automated kiwifruit counting technique. Image and Vision Computing New Zealand. In: 23rd International Conference, http://dx.doi.org/10.1109/IVCNZ.2008.4762149, <http://ieeexplore.ieee.org/stamp/stamp.jsp?tp=&arnumber=4762149&isnumber=4762060>, pp. 1–6.

Zhou, R., Damerow, L., et al., 2012. Using colour features of cv. 'Gala' apple fruits in an orchard in image processing to predict yield. Precision Agriculture 13 (5), 568–580.